

# Electrical and Magnetic Properties of Spinel Solid Solutions $\text{Mg}_{2-x}\text{Ti}_{1+x}\text{O}_4$ ; $0 \leq x \leq 1$

Heinrich Hohl,<sup>1</sup> Christian Kloc, and Ernst Bucher

Universität Konstanz, Fakultät für Physik, Postfach 5560, D-78434 Konstanz, Germany; and AT&T Bell Laboratories, P.O. Box 636, Murray Hill, New Jersey 07974

Received January 24, 1996; accepted May 30, 1996

Spinel solid solutions of composition  $\text{Mg}_{2-x}\text{Ti}_{1+x}\text{O}_4$  have been prepared and investigated in the range  $0 \leq x \leq 1$ . With increasing titanium content, the lattice parameter of the cubic unit cell increases from  $a = 844.00(3)$  pm to a maximum value of  $850.66(5)$  pm. Simultaneously, electrical properties evolve from insulating to low resistive semiconducting behavior. The resistivity of samples with compositions  $x \leq 0.68$  is thermally activated with activation energies above 70 meV. The magnetic properties of the solid solutions are mainly determined by a temperature dependent magnetic moment of  $\text{Ti}^{3+}$  in an octahedral crystal field. Reports about high- $T_c$  superconductivity in the solid solution series cannot be confirmed. © 1996 Academic Press, Inc.

Press, Inc.

## INTRODUCTION

*Spinel and high- $T_c$  superconductivity.* The discovery of high- $T_c$  superconductivity in copper oxide based perovskite-type materials (1) almost a decade ago was extraordinarily exciting for both science and possible technological applications and started an extensive search for further superconducting oxides. Whereas since then several dozen closely related copper oxide based superconductors with  $T_c$  values as high as 134 K (2) have been found, only four copper-free oxide superconductors with critical temperatures above 10 K are well established so far. These are  $\text{LiTi}_2\text{O}_4$  (3),  $\text{BaPb}_{0.75}\text{Bi}_{0.25}\text{O}_3$  (4),  $\text{Ba}_{0.6}\text{K}_{0.4}\text{BiO}_3$  (5), and  $\text{Sr}_{0.9}\text{Nd}_{0.1}\text{Nb}_2\text{O}_6$  (6) with critical temperatures of 13.7, 12, 30, and 11.5 K, respectively.

In 1991, Cogle (7) reported anomalous resistivity behavior reminiscent of transitions to superconductivity at about 50 K in  $\text{Mg}_{2-x}\text{Ti}_{1+x}\text{O}_4$  spinel solid solutions with titanium ions in an average oxidation state of 3.3–3.25 ( $x = 0.54$ – $0.6$ ). These observations were later strengthened by Namgung (8), Finch (9), and Kuzmicheva (10). The last study even speculates about superconducting inclusions with maximum critical temperatures near 150 K.

<sup>1</sup> To whom correspondence should be addressed.

A number of erroneous reports about new HTSCs during the past few years, the apparent instability of the reported resistivity anomalies, and the fact that no cross checking for superconductivity by magnetic measurements (Meissner or shielding effect) was performed by these groups give reason to regard the mentioned reports with a certain amount of suspicion. On the other hand, there are some aspects which let this spinel system indeed appear to be a potential candidate for high temperature superconductivity.

First, a common basic feature of oxide superconductors is that all are members (sometimes end members) of solid solutions which exhibit a metal/insulator transition upon compositional variation. Superconductivity generally occurs in the metallic regime close to the transition (11, 12). Second,  $\text{LiTi}_2\text{O}_4$  is a well-known example of a superconducting spinel whose properties rely on titanium ions with an average oxidation state between 3+ and 4+. A number of superconducting sulfo- and selenospinel (13) underline the compatibility between a spinel structure and the appearance of superconductivity. Finally, the  $x = 1$  member  $\text{MgTi}_2\text{O}_4$  features  $\text{Ti}^{3+}$  ions ( $S = 1/2$ ) in a three-dimensional pyrochlore (or B-site spinel) sublattice, an arrangement that tends to frustrate when occupied by spins with nearest neighbor antiferromagnetic interactions (14). This makes the  $\text{Mg}_{2-x}\text{Ti}_{1+x}\text{O}_4$  system also interesting with respect to Anderson's RVB theory of high temperature superconductivity (15), as the RVB state is favored by both low spin and magnetic frustration.

*Previous research.* The inverse spinel  $\text{Mg}_2\text{TiO}_4$  is a colorless insulator with a lattice parameter of  $a = 844.0$  pm (16). With all of the titanium ions in an oxidation state of 4+, the compound is readily prepared by a solid state reaction of the oxides in air. The normal spinel  $\text{MgTi}_2\text{O}_4$ , on the other hand, could not be prepared successfully so far. Lecerf claimed to have synthesized this compound (17), but later studies and the present work demonstrate that his sample was off-stoichiometric.

Feltz and Steinbrück (18) prepared  $\text{Mg}_{2-x}\text{Ti}_{1+x}\text{O}_4$  solid

solutions in the range  $0 \leq x \leq 0.93$  under inert conditions. The lattice parameter  $a$  was found to vary linearly with composition, and a value of  $a = (850.3 \pm 0.5)$  pm was estimated for the  $x = 1$  end member by extrapolation. Temperature dependent measurements of the resistivity revealed a continuous transition from insulating ( $x = 0$ ) to a low resistive semiconducting ( $x = 0.93$ ) behavior. Magnetic susceptibilities of  $x > 0$  solid solutions were analyzed in terms of Curie–Weiss behavior with Curie–Weiss temperatures between  $\Theta = -104$  K ( $x = 0.1$ ) and  $-1060$  K ( $x = 0.9$ ). Electrical and magnetic measurements were restricted to a temperature range of 77–340 K.

Cogle (7) studied the solid solution series in the range  $0 \leq x \leq 0.7$  and reports a similar dependence between  $a$  and  $x$ . With increasing titanium content, the room temperature resistivity of the samples was found to decrease ( $x \leq 0.54$ ), reach a minimum ( $x = 0.54$ – $0.6$ ) and then to increase again ( $x \geq 0.6$ ). Samples with  $x = 0.54$ – $0.6$  are reported to exhibit resistivity anomalies reminiscent of superconductivity at about 50 K. No magnetic investigations have been performed in the study.

**Research aim.** The forgoing text shows that bibliographic data leave several open questions concerning the properties of the spinel system  $\text{Mg}_{2-x}\text{Ti}_{1+x}\text{O}_4$ . Particularly the resistivity anomalies reported by Cogle call for a systematic and detailed study on this system. Furthermore, the magnetic data of Feltz and Steinbrück are difficult to understand as large negative Curie–Weiss temperatures in general indicate strong antiferromagnetic interactions between the magnetic ions. A transition into an ordered state is therefore to be expected at  $T \approx |\Theta|$  unless the system is frustrated. The aim of our work was to study the  $\text{Mg}_{2-x}\text{Ti}_{1+x}\text{O}_4$  spinel system in a systematic way in order to clarify these points.

## EXPERIMENTAL

**Synthesis.** Samples of composition  $\text{Mg}_{2-x}\text{Ti}_{1+x}\text{O}_4$  were prepared by solid state reactions of MgO (99.998%, Koch-Light Laboratories),  $\text{TiO}_2$  (99.95%, Atomergic Chemetals), and titanium powder (Fig. 1). The oxides were calcined at  $1000^\circ\text{C}$  before weighing to remove moisture. Titanium powder was filed off a Van Arkel titanium rod (99.9%, Koch-Light Laboratories) and checked for contamination with iron filings by means of a strong magnet. The chemicals were weighed in stoichiometric proportions, ground intimately in an agate mortar, and pressed to pellets of 10 mm diameter and 2 mm thickness by applying a pressure of  $10 \text{ kN/cm}^2$ .

In order to synthesize the  $x = 0$  compound, samples were placed into alumina boats and heated to temperatures of  $1250$ – $1450^\circ\text{C}$  for 16 h in air using a conventional tube furnace. Samples with an average titanium oxidation state below  $4+$  were piled up in an alumina vessel and annealed

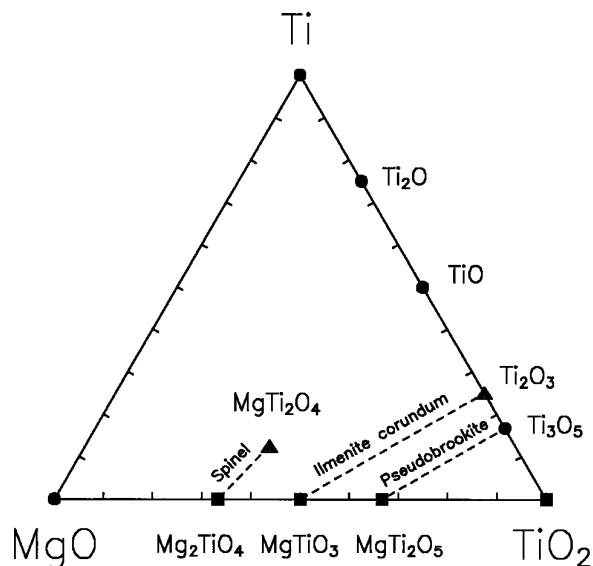


FIG. 1. Extract of the Mg–Ti–O phase diagram showing solid solutions with spinel, ilmenite corundum and pseudobrookite structure. Squares and triangles label tetravalent and trivalent titanium compounds, respectively.

to  $1400$ – $1450^\circ\text{C}$  for 1–4 h in argon atmosphere by inductive RF heating ( $\nu = 500 \text{ kHz}$ ). Tantalum foil was used in order to separate the samples from each other and to couple in RF power. The reaction temperature was measured with a pyrometer. All samples prepared under inert conditions were stored in an evacuated desiccator.

As in general it appears favorable to prepare oxide solid solutions by reaction of oxides solely, a batch of  $\text{Ti}_2\text{O}_3$  (99+%, Johnson Matthey) was purchased. Powder diffraction analysis and weight increase upon oxidation unveiled this batch as a mixture of  $\text{Ti}_2\text{O}_3$ , TiO, and  $\text{Ti}_2\text{O}$  with an overall composition of “ $\text{TiO}_{1.06}$ .” A few additional samples were prepared using this mixture of lower titanium oxides while considering its overall composition.

**Characterization.** The phase purity of the samples was determined using a Siemens D 5000 powder diffractometer equipped with a copper anode. A primary quartz monochromator was used to remove all but the  $\text{CuK}\alpha_1$  radiation. The diffractogram was recorded with a position sensitive detector, covering an angle of  $6^\circ$  with a resolution of  $0.01^\circ$ . Silicon powder was used as standard.

The resistivity was measured with the standard four-probe technique in the temperature range  $1.5$ – $300$  K. A carbon glass resistor (CGR) was used to determine the sample temperature. Indium contacts of  $0.2 \mu\text{m}$  thickness were evaporated to the samples and copper wires attached to them with silver epoxy.

Magnetic measurements were performed in the temperature range  $4.2$ – $300$  K with a Faraday–Curie magnetic balance. The temperature was measured with an AuFe/

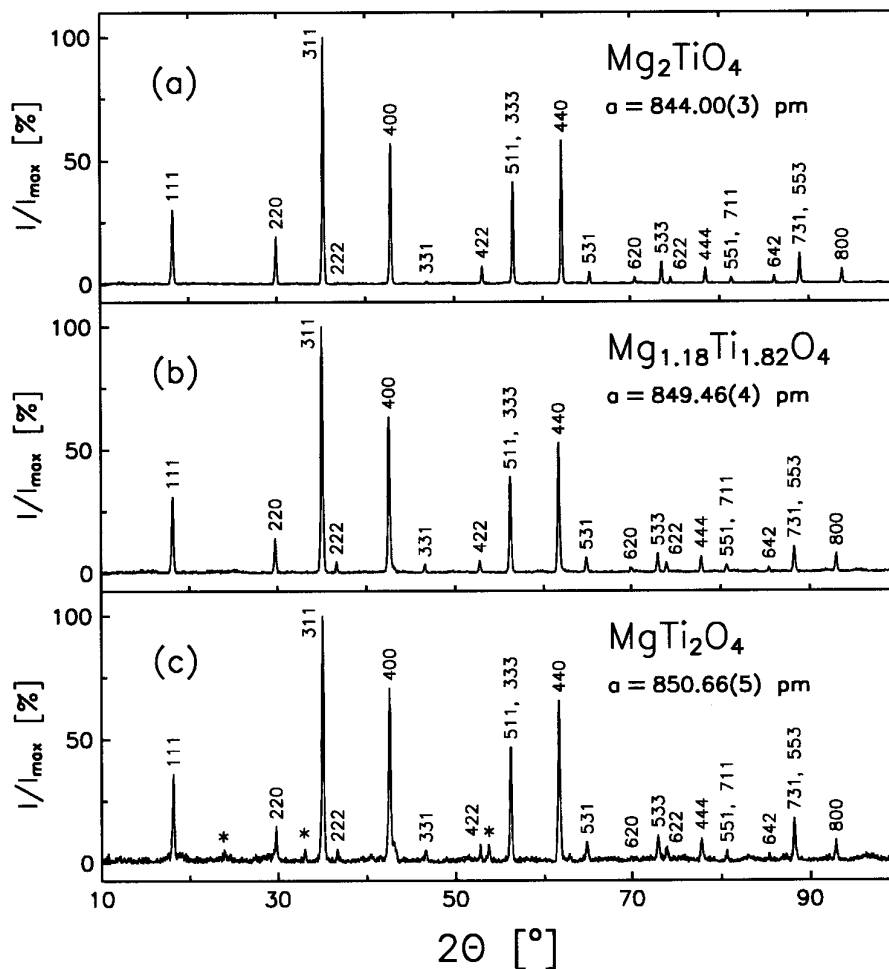


FIG. 2. Powder diffraction patterns of  $\text{Mg}_{2-x}\text{Ti}_{1+x}\text{O}_4$  samples, recorded with  $\text{CuK}\alpha$  radiation. Synthesis conditions: (a) 16 h at  $1325^\circ\text{C}$  in air, (b, c) 1 h at  $1400^\circ\text{C}$  in argon. Impurity phases: (\*)  $\text{Ti}_2\text{O}_3$ .

Chromel thermocouple, and fields of up to 8000 Oe were applied to the samples. The magnetic balance was calibrated using  $\text{HgCo}(\text{SCN})_4$  as standard.

## RESULTS AND DISCUSSION

**X-ray diffraction.** The inverse spinel  $\text{Mg}_2\text{TiO}_4$  ( $x = 0$ ) was prepared by solid state reaction of  $\text{MgO}$  and  $\text{TiO}_2$  in air. Reaction temperatures of at least  $1300^\circ\text{C}$  were necessary to obtain single phase material, whereas samples synthesized at lower temperatures contained noticeable amounts of  $\text{MgTiO}_3$  (geikielite). The lattice parameter of a sample synthesized at  $1325^\circ\text{C}$  was found to be  $a = 844.00(3)$  pm (Fig. 2a).

Mixtures of  $\text{MgO}$ ,  $\text{TiO}_2$ , and Ti (or “ $\text{TiO}_{1.06}$ ”), weighed according to nominal compositions  $\text{Mg}_{2-x}\text{Ti}_{1+x}\text{O}_4$  with  $x_n = 0-0.6$  and reacted for 1 h at  $1400^\circ\text{C}$  in argon, yielded phase pure solid solutions with lattice parameters between  $844.98(4)$  and  $849.46(4)$  pm. Mixtures with nominal compo-

sitions  $x_n = 0.66-0.76$  produced solid solutions with lattice parameters between  $849.79(6)$  and  $850.66(5)$  pm under the same conditions, but traces of  $\text{Ti}_2\text{O}_3$  were apparent in those samples. An even higher titanium content did not further increase the lattice parameter of the spinel solid solutions but rather raised the amount of the  $\text{Ti}_2\text{O}_3$  impurity phase. In contrast to the colorless  $x = 0$  compound synthesized in air, all samples reacted under inert conditions appeared dark black.

As variations in the sintering conditions (temperature and duration) markedly influenced the lattice parameters of the resulting spinel solid solutions, the lattice parameter  $a$  rather than  $x_n$  will be used to specify samples in this study. For more convenience the lattice parameters will be recalculated by a linear relation

$$x(a) = \frac{a/\text{pm} - 844.00}{6.66} \quad [1]$$

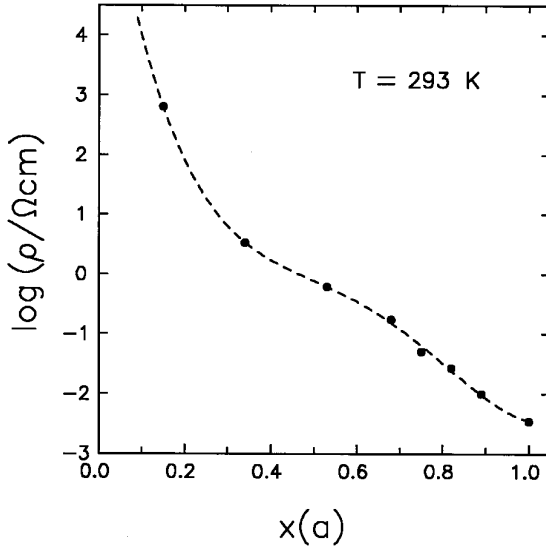


FIG. 3. Room temperature resistivity of  $\text{Mg}_{2-x}\text{Ti}_{1+x}\text{O}_4$  solid solutions as a function of the parameter  $x(a)$ . The dashed line is a guide for the eye.

which maps the set of lattice parameters obtained in the present study into an interval ranging from  $x(a_{\min}) = 0$  through  $x(a_{\max}) = 1$ . Here,  $a_{\min} = 844.00$  pm is the lattice parameter of the inverse spinel  $\text{Mg}_2\text{TiO}_4$ . Bearing in mind that the lattice parameter of  $\text{MgTi}_2\text{O}_4$  was estimated to be  $(850.3 \pm 0.5)$  pm by extrapolation (18), it seems justified to assign the saturation value  $a_{\max} = 850.66$  pm found in the present study to the  $x = 1$  end member of the spinel solid solution.<sup>2</sup> Values calculated by Eq. [1] are regarded as a good measure for the sample composition, since a linear variation of the lattice parameter with composition has been established by two groups (7, 18) in this system.

Powder diffraction patterns of samples with  $x = 0.82$  and  $x = 1.00$  are shown in Figs. 2b and 2c. Along with shifts in the peak positions, the transition from inverse to normal spinel structure with increasing titanium content causes changes in relative peak intensities, most apparent for the 220, 222, 331, and 622 reflections.

Due to a loss of Mg or MgO, reactions at  $1400^\circ\text{C}$  under inert conditions generally produced solid solutions with compositions  $x(a)$  about 20–25% higher than the nominal compositions  $x_n$  of the chemical mixtures. Similar observations are reported by other groups (8, 18) and manifest themselves in a weight loss and formation of  $\text{MgAl}_2\text{O}_4$  whiskers at the surface of the alumina vessels. A high reaction temperature, however, turns out to be an essential factor in the formation of  $\text{Mg}_{2-x}\text{Ti}_{1+x}\text{O}_4$  solid solutions with compositions close to  $x = 1$ . Samples reacted at  $1300^\circ\text{C}$  did not yield solid solutions with lattice parameters higher

<sup>2</sup> For comparison, maximum lattice parameters of  $850.2(2)$  and  $850.5(3)$  pm were reported by Lambert (19) and Johnston (20), respectively.

than  $849.00(4)$  pm, and  $\text{Mg}_{1-x}\text{Ti}_{1+x}\text{O}_3$  (21) impurities were present in those samples even at relatively low titanium contents.

*Electrical properties.* Samples of the inverse spinel  $\text{Mg}_2\text{TiO}_4$  reacted in air are insulating, as expected from the electronic configuration  $[\text{Ar}] 3d^0$  of the  $\text{Ti}^{4+}$  ions.

First measurements of the resistivity performed on samples with  $x > 0$  sometimes exhibited anomalies below 100 K due to contact problems. In the following all samples were polished with sand paper before contacts were attached, thus measuring the interior of the pellets rather than their surface. This additional treatment produced low resistive contacts and yielded very reproducible measurements.

Figure 3 shows the room temperature resistivity  $\rho(293\text{ K})$  of  $\text{Mg}_{2-x}\text{Ti}_{1+x}\text{O}_4$  solid solutions as a function of composition  $x(a)$ . The data points indicate a continuous transition from insulating ( $x = 0$ ) to low resistive semiconducting ( $x = 1$ ) behavior and confirm the results of Feltz and Steinbrück (18).

Temperature dependent resistivity measurements of  $\text{Mg}_{2-x}\text{Ti}_{1+x}\text{O}_4$  solid solutions are shown in Fig. 4. Samples with  $x \leq 0.68$  exhibit a thermally activated temperature dependence

$$\rho(T) = \rho_0 \exp\left(\frac{E_a}{k_B T}\right) \quad [2]$$

with activation energies  $E_a$  decreasing from 230 meV ( $x = 0.15$ ) to 115 meV ( $x = 0.68$ ). Above 200 K, samples

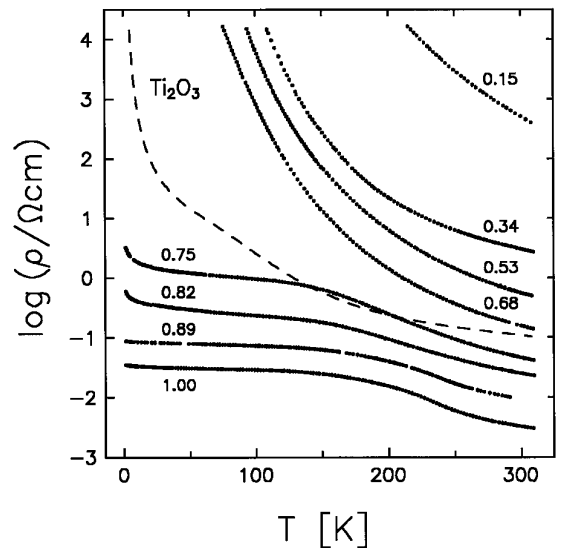


FIG. 4. Resistivity of  $\text{Mg}_{2-x}\text{Ti}_{1+x}\text{O}_4$  solid solutions in semi-logarithmic representation. The sample with  $x = 0$  is an insulator. A resistivity curve of  $\text{Ti}_2\text{O}_3$  is enclosed for comparison.

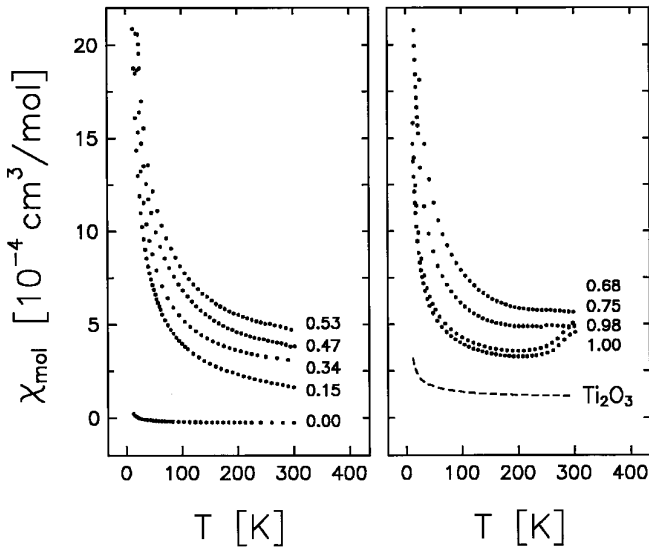


FIG. 5. Molar magnetic susceptibility of  $\text{Mg}_{2-x}\text{Ti}_{1+x}\text{O}_4$  solid solutions, measured in a magnetic field of  $H = 8$  kOe. A susceptibility curve of  $\text{Ti}_2\text{O}_3$  is enclosed for comparison.

with  $x = 0.75$  and  $0.82$  exhibit thermally activated behavior with  $E_a = 90$  and  $70$  meV, respectively, but the resistivity increase is less dramatic at lower temperatures. For  $x \geq 0.89$ , thermally activated behavior is apparent only above  $250$  K. None of the samples shows a transition to superconductivity or gives evidence for the presence of superconducting inclusions above  $1.5$  K.<sup>3</sup>

For the sake of comparison, Fig. 4 includes the resistivity curve of a single phase  $\text{Ti}_2\text{O}_3$  sample which was produced by reaction of Ti and  $\text{TiO}_2$  in an evacuated quartz ampoule at  $1300^\circ\text{C}$ . Thermally activated behavior with  $E_a = 43$  meV is found in the temperature range  $100$ – $325$  K, with a room temperature resistivity of  $1.1 \times 10^{-1} \Omega \text{ cm}$ . This agrees well with the literature data (23) and demonstrates that the relatively low resistivities found in  $\text{Mg}_{2-x}\text{Ti}_{1+x}\text{O}_4$  solid solutions with  $x \geq 0.75$  are not due to the presence of  $\text{Ti}_2\text{O}_3$  impurity phases.

**Magnetic properties.** All of the samples investigated in the present study revealed linear magnetization curves  $M = \chi_{\text{mol}}H$  at both room temperature and  $4.2$  K. The magnetic susceptibilities are shown in Fig. 5. All data are given in units of the electromagnetic cgs-system.

Due to the electronic configuration  $[\text{Ar}] 3d^0$  ( $L = S = 0$ ) of  $\text{Ti}^{4+}$ , only temperature-independent contributions to the magnetic susceptibility are present in the inverse spinel

<sup>3</sup> Kuzmicheva (10) assigned inflections like those seen in some resistivity curves of Fig. 4 below about  $200$  K to the presence of superconducting inclusions. Transitions between different major transport mechanisms, however, are basic phenomena in doped semiconductors (22) and appear to be a more plausible explanation for these anomalies.

TABLE 1  
Langevin Diamagnetic  
Susceptibilities of Ions  
(24)

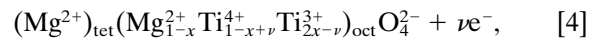
Ion	$\chi^{\text{dia}}$ [ $10^{-6} \text{ cm}^3/\text{mol}$ ]
$\text{Mg}^{2+}$	$-2.5$
$\text{Ti}^{4+}$	$-5$
$\text{Ti}^{3+}$	$-9.2$
$\text{O}^{2-}$	$-12$

$\text{Mg}_2\text{TiO}_4 = \text{Mg}_2^{2+}\text{Ti}^{4+}\text{O}_4^{2-}$ . Langevin diamagnetic susceptibilities of ions, determined empirically by Klemm (24), are given in Table 1 and add up to  $\chi^{\text{dia}} = -5.8 \times 10^{-5} \text{ cm}^3/\text{mol}$ . Additionally,  $\text{Ti}^{4+}$  in an octahedral environment of oxygen is known to exhibit a temperature-independent Van Vleck paramagnetism of  $\chi^{\text{VV}} = +3.3 \times 10^{-5} \text{ cm}^3/\text{mol}$  (25, 26), giving a total susceptibility of

$$\begin{aligned} \chi_0 &= \chi^{\text{dia}} + \chi^{\text{VV}} \\ &= -2.5 \times 10^{-5} \text{ cm}^3/\text{mol}. \end{aligned} \quad [3]$$

The value determined by experiment,  $\chi_0 = (-2.7 \pm 0.2) \times 10^{-5} \text{ cm}^3/\text{mol}$ , agrees well with this calculation and once more confirms the numerical value of  $\chi^{\text{VV}}$ .

For solid solutions with compositions  $0 < x \leq 1$ , the situation is more complex as additional magnetic contributions have to be taken into consideration. In a simple model,  $\text{Mg}_{2-x}\text{Ti}_{1+x}\text{O}_4$  may be written as



where  $\nu$  is the number of delocalized electrons per formula unit. The total magnetic susceptibility of the solid solutions is therefore given by

$$\chi_{\text{mol}}(T) = \chi^{\text{dia}} + \chi^{\text{VV}} + \chi^{\text{Ti}^{3+}}(T) + \chi^{\text{el}}(T). \quad [5]$$

Aside from the diamagnetic contributions  $\chi^{\text{dia}}$  provided by all of the ion cores and a Van Vleck paramagnetism  $\chi^{\text{VV}}$  caused by  $\text{Ti}^{4+}$  ions in an octahedral environment,  $\text{Ti}^{3+}$  with the electronic configuration  $[\text{Ar}] 3d^1$  ( $L = 2$ ,  $S = 1/2$ ) is expected to exhibit a permanent magnetic moment which gives reason for a temperature dependent contribution  $\chi^{\text{Ti}^{3+}}$ . Permanent magnetic moments usually manifest themselves in Curie-Weiss behavior  $C/(T - \Theta)$  of the magnetic susceptibility, where  $\Theta$  is a measure for the strength of magnetic interactions. As with other transition metal ions, the crystal field of surrounding anions may seriously influence the value of  $\mu_{\text{eff}}$ . Additionally, a delocalization of charge carriers according to  $\text{Ti}^{3+} \rightleftharpoons \text{Ti}^{4+} +$

**TABLE 2**  
Fit Parameters for the Magnetic Susceptibility of  $\text{Mg}_{1.85}\text{Ti}_{1.15}\text{O}_4$  in Different Temperature Regions

Temperature range [K]	$\chi_0$ [ $\text{cm}^3/\text{mol}$ ]	$C$ [ $\text{K cm}^3/\text{mol}$ ]	$\Theta$ [K]	$\mu_{\text{eff}}$ [ $\mu_{\text{B}}$ ]
10–50	$+1.76 \times 10^{-4}$	$2.52 \times 10^{-2}$	+0.1	0.82
50–100	$+7.12 \times 10^{-5}$	$3.46 \times 10^{-2}$	−6.3	0.96
100–150	$+3.98 \times 10^{-5}$	$4.14 \times 10^{-2}$	−16	1.05
150–300	$-1.45 \times 10^{-5}$	$6.59 \times 10^{-2}$	−67	1.32

*Note.* The effective magnetic moment  $\mu_{\text{eff}}$  per  $\text{Ti}^{3+}$  ion was calculated using Eq. [7] and the approximation  $z \approx 2x = 0.30$ .

$e^-$  is expected to cause electronic contributions  $\chi^{\text{el}}(T)$  to vary with temperature as does the carrier concentration,  $n(T)$ .

In solid solutions with compositions close to  $\text{Mg}_2\text{TiO}_4$ , the conductivity is low and  $\chi^{\text{el}}(T)$  may be neglected. Attempts to fit the magnetic susceptibility of  $\text{Mg}_{1.85}\text{Ti}_{1.15}\text{O}_4$  ( $x = 0.15$ ) in terms of a generalized Curie–Weiss law

$$\chi_{\text{mol}}(T) = \chi_0 + \frac{C}{T - \Theta} \quad [6]$$

in different temperature regions are displayed in Table 2. The obtained values of  $\chi_0$ ,  $C$ , and  $\Theta$  follow general trends which are also observed in samples with higher titanium content. Only a negligible Curie–Weiss temperature is apparent at low temperature. With increasing temperature,  $\Theta$  decreases monotonically and approaches a value of about  $-10^2$  K at room temperature. Simultaneously, an increase of the Curie constant indicates that the effective magnetic moment of  $\text{Ti}^{3+}$  in the solid solutions is temperature dependent.

The Curie constant of a substance, holding  $z$  equivalent ions with the magnetic moment  $\mu_{\text{eff}}$  per formula unit, is given by  $C = zN_{\text{A}}\mu_{\text{eff}}^2/3k_{\text{B}} = 0.125 (\mu_{\text{eff}}/\mu_{\text{B}})^2 \text{ K cm}^3/\text{mol}$ . An effective magnetic moment per  $\text{Ti}^{3+}$  ion may therefore be calculated from each Curie constant in Table 2 according to

$$\frac{\mu_{\text{eff}}}{\mu_{\text{B}}} = 2.828 \sqrt{\frac{C}{z} \frac{\text{mol}}{\text{K cm}^3}}. \quad [7]$$

The  $\mu_{\text{eff}}$  data listed in Table 2 are based on the approximation  $z \approx 2x$ , thereby completely ignoring the formation of charge carriers suggested by Eq. [4].

In order to analyze the temperature dependence of the effective magnetic moment in an extended temperature range, we make use of the basic relation between  $\mu_{\text{eff}}$  and  $\chi^{\text{Ti}^{3+}}(T)$ ,

$$\frac{\mu_{\text{eff}}}{\mu_{\text{B}}} = 2.828 \sqrt{\frac{\chi^{\text{Ti}^{3+}}(T) \times T \frac{\text{mol}}{\text{K cm}^3}}{z}}. \quad [8]$$

Approximating  $\chi^{\text{el}} \approx 0$  and  $z \approx 2x$ , we have  $\chi^{\text{Ti}^{3+}}(T) \approx \chi_{\text{mol}}(T) - \chi_0$ , where the sum of temperature-independent contributions to the magnetic susceptibility is given by  $\chi_0(x) = -(2.5 + 4.4x) \times 10^{-5} \text{ cm}^3/\text{mol}$ . A plot of  $\mu_{\text{eff}}$  vs  $T$  for the  $x = 0.15$  sample is shown in Fig. 6 and clearly shows the temperature dependence of the effective magnetic moment.

For a quantitative analysis, we discuss the magnetic behavior of  $\text{Ti}^{3+}$  in an octahedral crystal field as predicted by theory (27). Under the influence of the crystal field, the 10-fold degenerate  ${}^2D$  energy level of  $\text{Ti}^{3+}$  splits into a 4-fold degenerate  ${}^2E_g$  term and a 6-fold degenerate  ${}^2T_{2g}$  term. Only the latter is of importance for the magnetic behavior under laboratory conditions. Considering further splitting of the  ${}^2T_{2g}$  term due to spin–orbit coupling and the presence of a magnetic field, Van Vleck’s equation predicts a magnetic susceptibility which may be written as

$$\chi^{\text{Ti}^{3+}}(T) = N_{\text{A}} \frac{\mu_{\text{eff}}^2}{3k_{\text{B}}T}, \quad [9]$$

with a temperature dependent effective magnetic moment

$$\mu_{\text{eff}}^2 = \frac{8 + (3\xi - 8) \exp(-\frac{3}{2}\xi)}{\xi[2 + \exp(-\frac{3}{2}\xi)]} \mu_{\text{B}}^2 \quad [10]$$

and a dimensionless parameter  $\xi = \lambda/k_{\text{B}}T$ . The quantity

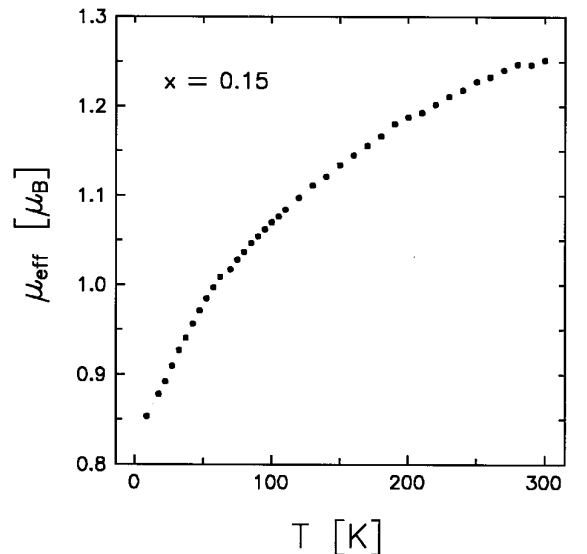


**FIG. 6.** Temperature dependence of the effective magnetic moment per  $\text{Ti}^{3+}$  ion in  $\text{Mg}_{1.85}\text{Ti}_{1.15}\text{O}_4$ , calculated using Eq. [8] and the approximations  $\chi^{\text{el}} \approx 0$ ,  $z \approx 2x$ .

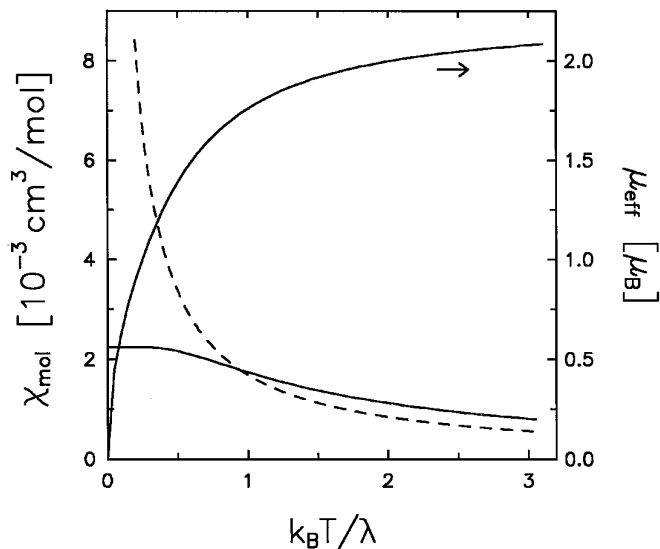


FIG. 7. Molar magnetic susceptibility and effective magnetic moment  $\mu_{\text{eff}}$  of octahedrally coordinated  $\text{Ti}^{3+}$  as a function of  $k_{\text{B}}T/\lambda$ . The dashed line corresponds to a temperature-independent magnetic moment of  $\mu_{\text{eff}}^{\text{S.O.}} = 1.73 \mu_{\text{B}}$ .

$\lambda$  is the spin-orbit coupling parameter of  $\text{Ti}^{3+}$  when the ion is embedded in the crystal lattice.

Figure 7 shows the theoretically predicted magnetic susceptibility and effective magnetic moment of octahedrally coordinated  $\text{Ti}^{3+}$  plotted versus  $\xi^{-1} = k_{\text{B}}T/\lambda$  ( $\xi^{-1}$  represents a temperature scale in units of 223 K if the free-ion value of the spin-orbit coupling parameter,  $\lambda = 155 \text{ cm}^{-1}$ , is used). The behavior of the magnetic susceptibility is characterized by a transition from temperature-independent Van Vleck paramagnetism at low temperature ( $\xi^{-1} \ll 1$ ) to Curie-Weiss-like behavior at high temperature ( $\xi^{-1} \gg 1$ ). The effective magnetic moment increases from  $\mu_{\text{eff}}^0 = 0$  at  $T = 0$ , where magnetic moments of spin and orbit compensate each other, through a spin-only value  $\mu_{\text{eff}}^{\text{S.O.}} = [S(S+1)]^{1/2} \mu_{\text{B}} = 1.73 \mu_{\text{B}}$  near room temperature, and approaches a saturation value of  $\mu_{\text{eff}}^{\infty} = [L(L+1) + 4S(S+1)]^{1/2} \mu_{\text{B}} = 2.24 \mu_{\text{B}}$  at high temperature, where the magnetic moments of spin and orbit maximally enhance each other.<sup>4</sup>

It is important to point out that the Curie-Weiss like behavior observed at high temperature, with Curie-Weiss temperatures on the order of  $-10^2 \text{ K}$ , is purely artificial. Large negative values of  $\Theta$  are often associated with the presence of antiferromagnetic interactions, but such an interpretation may be misleading in general as no magnetic interactions were assumed to derive Eq. [9].

<sup>4</sup> Due to its 3-fold degeneracy with respect to the orbital momentum, the  ${}^2T_{2g}$  ground term behaves like a P state with  $L = 1$  in the cases just mentioned (24).

Even though Eq. [9] permits an understanding of the temperature dependence of the magnetic moment of  $\text{Ti}^{3+}$  in principle, this relation is not sufficient to describe the magnetic behavior of any known  $\text{Ti}^{3+}$  compound quantitatively. The magnetic moment of  $\text{CsTi}(\text{SO}_4)_2 \cdot 12 \text{ H}_2\text{O}$  (28), for instance, varies much less dramatically with temperature than predicted by Eq. [10] due to a slight trigonal distortion of the octahedral environment around  $\text{Ti}^{3+}$ . The fact that anion parameters of real spinel compounds generally deviate from the ideal value  $u = 3/8$ ,<sup>5</sup> and octahedra formed by the anions therefore exhibit a trigonal distortion along the  $\langle 111 \rangle$  direction of the cubic unit cell, suggest that the relatively modest temperature dependence of  $\mu_{\text{eff}}$  in Fig. 6 is also caused by a nonideal spinel structure.

Since the formation of charge carriers was neglected in Fig. 6, actual values of  $\mu_{\text{eff}}$  are expected to be somewhat higher than displayed in this plot. By comparing the data in Fig. 6 with those reported for the insulator  $\text{CsTi}(\text{SO}_4)_2 \cdot 12 \text{ H}_2\text{O}$ , a ratio of about 0.7 is found. Consequently, only  $\chi^{\text{el}} \approx 0$  proves to be a good approximation for compositions  $x \ll 1$ , whereas  $z \approx 2x$  had to be replaced by  $z = 2x - \nu$  with  $\nu \approx x$  even for a doping level as low as  $x = 0.15$ .

Electronic contributions  $\chi^{\text{el}}(T)$  to the magnetic susceptibility become more important at higher titanium content, where  $\chi^{\text{Ti}^{3+}}(T)$  loses some of its weight, as seen in the right portion of Fig. 5.<sup>6</sup> A detailed analysis of  $\chi^{\text{el}}(T)$  is complicated and lies beyond scope of this study. In general, aside from the effective mass  $m$  of charge carriers and their temperature-dependent concentration  $n(T)$ , the system's degree of degeneracy  $\alpha = (E_{\text{F}} - E_{\text{C}})/k_{\text{B}}T$  had to be taken into account for such an analysis (31). For this reason, only an estimation for the magnitude of  $\chi^{\text{el}}$  in  $\text{MgTi}_2\text{O}_4$  will be given in conclusion.

Assuming  $\nu = 1$  charge carrier per formula unit, equivalent to a carrier concentration of  $n = 8/a^3 = 1.3 \times 10^{22} \text{ cm}^{-3}$ , and an effective mass of  $m = 9.4 m_{\text{e}}$  as found in  $\text{LiTi}_2\text{O}_4$  (30), a magnetic susceptibility of  $\chi^{\text{el}} \approx +2 \times 10^{-4} \text{ cm}^3/\text{mol}$  has to be expected in the limit of strong degeneracy. With this order of magnitude,  $\chi^{\text{el}}(T)$  might be an explanation for the increase in the magnetic susceptibility observed in samples with  $x = 0.98$  and  $1.0$  between 250 and 300 K (Fig. 5). A susceptibility curve of  $\text{Ti}_2\text{O}_3$  is included in Fig. 5 for comparison and proves that these anomalies are not likely to be caused by traces of  $\text{Ti}_2\text{O}_3$ . In addition, no other lower oxides of titanium are known to exhibit susceptibility anomalies near the temperature range in question (32).

<sup>5</sup> Anion parameters of real spinels vary in the range  $0.36 \leq u \leq 0.40$  (29). An anion parameter of  $u = 0.3895$  was determined for  $\text{LiTi}_2\text{O}_4$  by Johnston (30).

<sup>6</sup> For comparison,  $\text{Li}_{1+x}\text{Ti}_{2-x}\text{O}_4$  solid solutions approach a metallic state with negligible magnetic contributions  $\chi^{\text{Ti}^{3+}}(T)$  in the limit  $x = 0$  (30).

## CONCLUSIONS

Spinel solid solutions of composition  $\text{Mg}_{2-x}\text{Ti}_{1+x}\text{O}_4$  have been prepared and investigated in the full range  $0 \leq x \leq 1$  for the first time. A high reaction temperature of  $1400^\circ\text{C}$  and Mg excess are essential factors in the formation of solid solutions with compositions close to  $x = 1$ . No marked differences in phase purity and physical properties were found between samples prepared using titanium powder and those based on a “ $\text{TiO}_{1.06}$ ” oxide mixture.

A continuous transition from insulating ( $x = 0$ ) to low resistive semiconducting ( $x = 1$ ) behavior is found in the solid solution series. The temperature dependence of the resistivity is thermally activated with activation energies above 70 meV. No resistivity anomalies reminiscent of transitions to superconductivity were observed at low temperature after careful attachment of electrical contacts. Neither do magnetic measurements give evidence for the presence of superconducting inclusions in the samples.

In order to analyze the magnetic properties of the solid solutions, a temperature-dependent magnetic moment  $\mu_{\text{eff}}$  for the  $\text{Ti}^{3+}$  ions was taken into account. The temperature dependence of  $\mu_{\text{eff}}$  indicates a deviation of the spinel structure's anion parameter from the ideal value  $u = 3/8$ . Previous studies of the magnetic properties of  $\text{Ti}^{3+}$  have mainly concentrated on cesium titanium sulfate  $\text{CsTi}(\text{SO}_4)_2 \cdot 12 \text{H}_2\text{O}$ . The results of our measurements demonstrate that oxide systems like  $\text{Mg}_{2-x}\text{Ti}_{1+x}\text{O}_4$ ,  $\text{Mg}_{1-x}\text{Ti}_{1+x}\text{O}_3$  (21),  $\text{SrTiO}_{3-\delta}$  (25),  $\text{TiO}_{2-\delta}$  (26), and  $\text{Mg}_{1-x}\text{Ti}_{2+x}\text{O}_5$  (33) are also promising substances for studies on the magnetic behavior of  $\text{Ti}^{3+}$  in a crystal field.

## ACKNOWLEDGEMENTS

It is a pleasure to thank C. S. Oglesby, B. Batlogg, and A. P. Ramirez for helpful discussions.

## REFERENCES

1. J. G. Bednorz and K. A. Müller, *Z. Phys. B* **64**, 189 (1986).
2. E. V. Antipov, S. M. Laureiro, C. Chaillout, J. J. Capponi, P. Bordet, J. L. Tholence, S. N. Putilin, and M. Marezio, *Physica C* **215**, 1 (1993).
3. D. C. Johnston, H. Prakash, W. H. Zachariasen, and R. Viswanathan, *Mater. Res. Bull.* **8**, 777 (1973).
4. A. W. Sleight, J. L. Gillson, and P. E. Bierstedt, *Solid State Commun.* **17**, 27 (1975).
5. R. J. Cava, B. Batlogg, J. J. Krajewski, R. Farrow, L. W. Rupp, A. E. White, K. Short, W. F. Peck, and T. Kometani, *Nature* **332**, 814 (1988).
6. J. Akimitsu, J. Amano, H. Sawa, O. Nagase, K. Gyoda, and M. Kogai, *Jpn. J. Appl. Phys.* **30**, L1155 (1991).
7. T. J. Cogle, C. A. S. Mateus, J. H. Binks, and J. T. S. Irvine, *J. Mater. Chem.* **1**, 289 (1991).
8. C. Namgung, A. B. Sheikh, A. A. Finch, and J. T. S. Irvine, *Appl. Supercond.* **1**, 511 (1993).
9. A. A. Finch, A. B. Sheikh, C. Namgung, and J. T. S. Irvine, “Proc. 5th Int. Symp. Supercond., Kobe, Japan, November 1992.”
10. G. M. Kuzmicheva and A. V. Mittin, *Russ. J. Inorg. Chem.* **40**, 851 (1995).
11. R. J. Cava, B. Batlogg, J. J. Krajewski, W. F. Peck, and L. W. Rupp, *J. Less-Common Met.* **164 & 165**, 749 (1990).
12. H. Hohl, “Oxidische Supraleiter und verwandte Systeme,” Ph.D. Thesis, Hartung Gorre-Verlag, Konstanz, 1995.
13. N. H. van Maaren, G. M. Schaeffer, and F. K. Lotgering, *Phys. Lett. A* **25**, 238 (1967).
14. A. P. Ramirez, *Ann. Rev. Mater. Sci.* **24**, 453 (1994).
15. P. W. Anderson, *Science* **235**, 1194 (1987).
16. B. A. Wechsler and A. Navrotsky, *J. Solid State Chem.* **55**, 165 (1984).
17. A. Lecerf, *Ann. Chim.* **7**, 513 (1962).
18. A. Feltz und M. Steinbrück, *J. Less-Common Met.* **167**, 233 (1991).
19. P. M. Lambert, M. R. Harrison, and P. P. Edwards, *J. Solid State Chem.* **75**, 332 (1988).
20. D. C. Johnston, Ph.D. Thesis, University of California, San Diego, 1975.
21. A. Feltz und M. Steinbrück, *Z. Anorg. Allg. Chem.* **590**, 137 (1990).
22. B. I. Shklovskii and A. L. Efros, “Electronic Properties of Doped Semiconductors.” Springer-Verlag, Berlin/Heidelberg, 1984.
23. J. Yahia and H. P. R. Frederikse, *Phys. Rev.* **123**, 1257 (1961).
24. A. Weiss and H. Witte, “Magnetochemie.” Verlag Chemie, Weinheim, 1973.
25. H. P. R. Frederikse and G. A. Candela, *Phys. Rev.* **147**, 583 (1966).
26. F. E. Senftle and A. N. Thorpe, *Phys. Rev.* **175**, 1144 (1968).
27. F. E. Mabbs and D. J. Machin, “Magnetism and Transition Metal Complexes.” Chapman and Hall, London, 1973.
28. B. N. Figgis, J. Lewis, and F. E. Mabbs, *J. Chem. Soc.* **63**, 2473 (1963).
29. F. S. Galasso, “Structure and Properties of Inorganic Solids.” Pergamon, Oxford, 1970.
30. D. C. Johnston, *J. Low Temp. Phys.* **25**, 145 (1976).
31. G. Busch, A. Menth und B. Natterer, *Z. Naturforsch. A* **19**, 542 (1964).
32. A. D. Pearson, *J. Phys. Chem. Solids* **5**, 316 (1958).
33. A. Feltz und M. Steinbrück, *Z. Anorg. Allg. Chem.* **594**, 157 (1991).